J/Ψ suppression in colliding nuclei: statistical model analysis

Dariusz Prorok and Ludwik Turko
Institute of Theoretical Physics, University of Wrocław,
Pl. Maksa Borna 9, 50-204 Wrocław, Poland
(December 27, 2000)

We consider the J/Ψ suppression at a high energy heavy ion collision. An ideal gas of massive hadrons in thermal and chemical equilibrium is formed in the central region. The finite-size gas expands longitudinally in accordance with Bjorken law. The transverse expansion in a form of the rarefaction wave is taken into account. We show that J/Ψ suppression in such an environment, when combined with the disintegration in nuclear matter, gives correct evaluation of NA38 and NA50 data in a broad range of initial energy densities.

PACS: 14.40.Lb, 24.10Pa, 25.75.-q

I. INTRODUCTION

Since the paper of Matsui and Satz [1] there is a steady interest in the problem of J/Ψ suppression in a heavy-ion collision. The question is if this suppression can be treated as a signature for a quark-gluon plasma (QGP) or if it can be explained by J/Ψ absorption in a hadron gas which appears instead of the QGP in the central rapidity region (CRR) of the collision [2–6]. In the following paper we shall explore the latter possibility.

The existence of the QGP — the novel phase of hadron matter, has been predicted upon lattice QCD calculations (for a review see [7] and references therein). One gets from those calculations the critical temperature T_c in the range of 150 - 270 MeV. The upper limit belongs to a pure $SU(3)$ theory, whereas adding quarks causes lowering of T_c even to about 150 MeV ($N_f \geq 3$). All lattice calculations have been performed for zero quark and baryon chemical potential only. Additionally to the fact that lattice estimations could not be treated literally, in relativistic heavy ion collisions there is a finite baryon chemical potential. As a result, the above-mentioned evaluations of T_c can be understood only as a measure of the order of the magnitude of real T_c. Therefore, the assumption that at initial temperatures around 200 MeV (as in our model) a hadron gas still exists is realistic entirely. As far as the hadron gas is considered itself in that range of temperature, it was shown in [8] that the temperature increases with energy density when continuum excitations (string degrees of freedom) are not taken into account. Continuum excitations gives the limiting temperature. This reproduces results of the Hagedorn bootstrap model [9]. The thermodynamical analysis can also be based on particle ratios [10] and this gives the temperature as in our model. The same result is obtained from the microscopic cascade model (see e.g. [11]).

In the following paper we shall continue our previous investigations [12] into the problem of J/Ψ suppression observed in a heavy-ion collision (for experimental data see e.g. [13,14] and references therein). Now, we shall focus on the dependence of the suppression on the initial energy density reached in the CRR.

In our model, J/Ψ suppression is the result of a $c\bar{c}$ state absorption in a dense hadronic matter through interactions of the type

$$c\bar{c} + h \longrightarrow D + \bar{D} + X, \tag{1}$$

where h denotes a hadron, D is a charm meson and X means a particle which is necessary to conserve the charge, baryon number or strangeness.

First, the J/Ψ is absorbed by nucleons in colliding nuclei [15]. Later, the J/Ψ is absorbed by secondary hadrons produced in the collision. In the simpler scenario those secondary hadrons expand longitudinally along collision axis [16,17] and the time evolution is given by Bjorken's scaling dynamics [18]. The importance of secondaries scattering becomes more and more important at higher energies since secondary production grows with energy as well. We assume that at very high energies secondaries form a dense hadronic gas in a state of thermodynamical equilibrium. A chemistry will be given by equation of state of an ideal gas consisting of different species of massive hadrons.

A problem of thermal and chemical equilibration of an hadronic fireball formatted in a heavy collision is still far from being solved. Recent results [11,8,19], based on parton cascade models, suggest that in big systems the equilibration time for heavier particles is longer than for lighter particles. The thermal equilibrium is established quickly, in about 5 fm/c, much faster than the chemical equilibrium.

To keep our model as simple as possible we consider the one temperature model. This allows us to reduce the number of external parameters. It is obvious that any new parameter would result in a better fit to experimental data.

The hadronic matter is in a state of an ideal gas of massive hadrons in thermal and chemical equilibrium and consists of all species up to Ω^- baryon. Time evolution is given here by conservation laws combined with assumptions about the space-time structure of the system. A corresponding equation of state of the ideal gas makes then possible to express gas parameters such as temperature and chemical potentials as functions of time.

An ideal gas of real hadrons has a very interesting feature: it cools much slower than a pion gas when expands longitudinally. We have checked numerically that for the initial energy densities ϵ_0 corresponding to initial temperatures T_0 of the order of 200 MeV and for the freeze-out $T_{f.o.}$ not lower than about 100 MeV, the time dependence of the temperature of the expanding gas still keeps the well-known form $T(t) = T_0 \cdot t^{-a}$ (we put $t_0 = 1$ fm). Only the exponent a changes from $\frac{1}{3}$ for massless pions to the values $\frac{1}{5.6}$-$\frac{1}{5.3}$ for massive realistic hadrons. As a result, the time of the freeze-out $t_{f.o}$ is much greater for the hadron gas than for the pion one. For instance, when we take $T_0 = 200$ MeV and $T_{f.o.} = 140$ MeV we obtain $t_{f.o.} = 7.37$ fm ($a = \frac{1}{5.6}$) for the hadron gas and $t_{f.o.} = 2.9$ fm ($a = \frac{1}{3}$) for the pion gas. The lower $T_{f.o.}$, the stronger difference. For $T_0 = 200$ MeV and $T_{f.o.} = 100$ MeV we have $t_{f.o.} = 48.5$ fm ($a = \frac{1}{5.6}$) for the hadron gas and $t_{f.o.} = 8$ fm ($a = \frac{1}{3}$) for the pion gas. This has a direct consequence for J/Ψ suppression: the longer the system lasts, the deeper suppression causes (see Fig. 1).

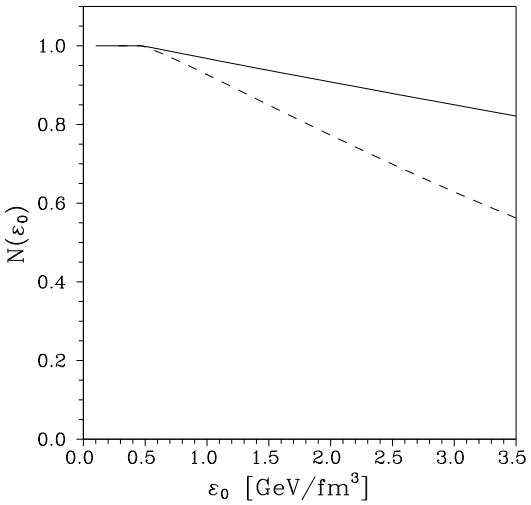

FIG. 1. Comparison of suppression of the pure J/Ψ's in the cooling hadron gas for two values of the power a in approximation $T(t) \cong T_0 \cdot t^{-a}$: $a = \frac{1}{3}$ (solid) and $a = \frac{1}{5.6}$ (dashed).

We are going to calculate a survival factor for J/Ψ when new, more realistic conditions are taken into account. We consider a hadronic gas which is produced in the CRR region. This gas expands both longitudinally and transversely. The longitudinal expansion is a traditional adiabatic hydrodynamical evolution [18], the transverse expansion is considered as the rarefaction wave. An initial energy density depends now on the impact parameter b and on the geometry of the collision.

The concept of the description of J/Ψ absorption in the hot hadronic matter is based on the application of the relativistic kinetic equation as it was postulated in [5]. As the hadronic medium a pion gas was taken into account there. Our hadronic medium consists of hadrons from the lowest up to Ω^- as constituents of the matter in the CRR. This gives different physical properties important for the absorption processes as compared to the absorption in a pion gas — cooling time, threshold effects, etc. It allows us to consider here also a case with non-zero baryon number density. We take into account here some physical effects which were neglected or not fully treated in [5]. Thresholds for $J/\Psi - hadron$ reactions as well as relative velocities are examined completely, but both these effects are ignored in final calculations in [5]. In addition to the CRR also J/Ψ absorption in the nuclear matter is considered simultaneously here. In the final estimations of J/Ψ survival fraction, the Woods-Saxon nuclear matter density distribution is used in the presented model.

As far as the hydrodynamic is concerned, the full solution of hydrodynamic equations (for the baryon number density equal to zero) with the use of the method developed in [20] was explored in [5], but with different initial temperature profile. Here, for simplicity of numerical calculations we assumed the uniform initial temperature distribution with the sharp edge at the border established by nuclei radii (see Fig. 2). For such an initial

distribution, and for a central collision and the baryon number density equal to zero, hydrodynamic equations are solved numerically in [20]. The resulting evolution can be decomposed into the longitudinal expansion inside a slice bordered by the front of the rarefaction wave and the transverse expansion which is superimposed outside of the wave. But the temperature decreases very quickly outside the wave (at least at times not greater than the half of the freeze-out time), so it is reasonable to ignore the influence of the flow outside of the rarefaction wave as we do in our model. Since we are dealing with small but nevertheless non-zero baryon number densities, we assume that the full hydrodynamic evolution looks like the same in this case. For the longitudinal expansion — the most important part of the hydrodynamical evolution, this assumption is confirmed by our investigations into the time dependence of the temperature of the hadron gas, where the same pattern (see (22)) has been obtained approximately as in the case of a massless baryonless ideal gas [21,22].

The dependence of J/Ψ suppression on the impact parameter b is treated here more rigorously than in [5]. In fact the only approximation of the survival factor (with respect to its exact expression for the case of the finite-size effects and the transverse expansion taken into account) is done by treating the time J/Ψ needs to escape from the hadron matter in the transverse plane on the average (over the initial J/Ψ positions). The effective freeze-out time t_f (denoted by t_{final} herein) is therefore the function of both the impact parameter and J/Ψ transverse momentum, whereas t_f is evaluated only for given b (for some assumed average J/Ψ transverse momentum, namely equal to 1 GeV) in [5].

II. THE EXPANDING HADRON GAS

For an ideal hadron gas in thermal and chemical equilibrium, which consists of l species of particles, energy density ϵ, baryon number density n_B, strangeness density n_S and entropy density s read ($\hbar = c = 1$ always)

$$\epsilon = \frac{1}{2\pi^2}\sum_{i=1}^{l}(2s_i+1)\int_0^\infty dp\,\frac{p^2 E_i}{\exp\left\{\frac{E_i-\mu_i}{T}\right\}+g_i}\ , \tag{2a}$$

$$n_B = \frac{1}{2\pi^2}\sum_{i=1}^{l}(2s_i+1)\int_0^\infty dp\,\frac{p^2 B_i}{\exp\left\{\frac{E_i-\mu_i}{T}\right\}+g_i}\ , \tag{2b}$$

$$n_S = \frac{1}{2\pi^2}\sum_{i=1}^{l}(2s_i+1)\int_0^\infty dp\,\frac{p^2 S_i}{\exp\left\{\frac{E_i-\mu_i}{T}\right\}+g_i}\ , \tag{2c}$$

$$s = \frac{1}{6\pi^2 T^2}\sum_{i=1}^{l}(2s_i+1)\int_0^\infty dp\,\frac{p^4}{E_i}\frac{(E_i-\mu_i)\exp\left\{\frac{E_i-\mu_i}{T}\right\}}{\left(\exp\left\{\frac{E_i-\mu_i}{T}\right\}+g_i\right)^2}\ , \tag{2d}$$

where $E_i = (m_i^2+p^2)^{1/2}$ and m_i, B_i, S_i, μ_i, s_i and g_i are the mass, baryon number, strangeness, chemical potential, spin and a statistical factor of specie i respectively (we treat an antiparticle as a different specie). And $\mu_i = B_i\mu_B + S_i\mu_S$, where μ_B and μ_S are overall baryon number and strangeness chemical potentials respectively.

We shall work here within the usual timetable of the events in the CRR of a given ion collision (for more details see e.g. [5]). We fix $t = 0$ at the moment of the maximal overlap of the nuclei. After half of the time the nuclei need to cross each other, matter appears in the CRR. We assume that soon thereafter matter thermalizes and this moment, t_0, is estimated at about 1 fm [5,18]. Then matter starts to expand and cool and after reaching the freeze-out temperature it is no longer a thermodynamical system. We denote this moment as $t_{f.o.}$. As we have already mentioned in the introduction, this matter is the hadron gas, which consists of all hadrons up to Ω^- baryon. The expansion proceeds according to the relativistic hydrodynamic equations and for the longitudinal component we have the following solution (for details see e.g. [18,23])

$$s(t) = \frac{s_0 t_0}{t}\ , \qquad n_B(t) = \frac{n_B^0 t_0}{t}\ , \tag{3}$$

where s_0 and n_B^0 are initial densities of the entropy and the baryon number respectively. The superimposed transverse expansion has the form of the rarefaction wave moving radially inward with a sound velocity c_s and the transverse flow which starts outside the wave [18,20]. But as it has been mentioned in the introduction, since the temperature decreases rapidly outside the wave (for the most important times for absorption processes), we shall ignore possible J/Ψ scattering there. It means that J/Ψ suppression is slightly underestimated here.

To obtain the time dependence of temperature and baryon number and strangeness chemical potentials one has to solve numerically equations (2b - 2d) with s, n_B and n_S given as time dependent quantities. For $s(t)$, $n_B(t)$ we have expressions (3) and $n_S = 0$ since we put the overall strangeness equal to zero during all the evolution (for more details see [21]).

The sound velocity squared is given by $c_s^2 = \frac{\partial P}{\partial \epsilon}$ and can be evaluated numerically [21,22].

III. J/Ψ ABSORPTION IN HADRONIC MATTER

In a high energy heavy-ion collision, charmonium states are produced mainly through gluon fusion and it takes place during the overlap of colliding nuclei. For the purpose of our model, we shall assume that all $c\bar{c}$ pairs are created at the moment $t = 0$. Before the fusion, gluons can suffer multiple elastic scattering on nucleons and gain some additional transverse momentum in this way [24–26]. This manifests for instance in the observed broadening of the p_T distribution of J/Ψ [27]. Following [28], we express this effect by the transverse momentum distribution of the charmonium states

$$g(p_T, \epsilon_0) = \frac{2p_T}{\langle p_T^2 \rangle^{AB}_{J/\Psi}(\epsilon_0)} \cdot \exp\left\{ -\frac{p_T^2}{\langle p_T^2 \rangle^{AB}_{J/\Psi}(\epsilon_0)} \right\} , \tag{4}$$

where $\langle p_T^2 \rangle^{AB}_{J/\Psi}(\epsilon_0)$ is the mean squared transverse momentum of J/Ψ gained in an A-B collision with the initial energy density ϵ_0. The momentum can be expressed as (for details see [29])

$$\langle p_T^2 \rangle^{AB}_{J/\Psi}(\epsilon) = \langle p_T^2 \rangle^{pp}_{J/\Psi} + K \cdot \epsilon , \tag{5}$$

with $K = 0.27$ fm^{3}GeV and $\langle p_T^2 \rangle^{pp}_{J/\Psi} = 1.24$ GeV^2 taken from a fit to the J/Ψ data of NA38 Collaboration [29]. The expression in (4) is normalized to unity and is treated as the initial momentum distribution of charmonium states here.

For the simplicity of our model, we shall assume that all charmonium states are completely formed and can be absorbed by the constituents of a surrounding medium from the moment of creation. It means that we neglect a whole complex process of J/Ψ formation as presented in [30,31]. The main feature of the above-mentioned process is that, soon after the moment of production, the $c\bar{c}$ pair binds a soft gluon and creates a pre-resonance $c\bar{c} - g$ state, from which, after a time of the order of 0.3 fm, a physical charmonium state is formed. This means that the possible nuclear absorption of charmonium is, in fact, the absorption of the $c\bar{c} - g$ state. But the latest has the cross-section $\sigma_{abs} = 7.3$ mb, which is much higher than $J/\Psi - Nucleon$ absorption cross-section $\sigma_{\psi N} \cong 3 - 5$ mb obtained from p-A data [15,27,32]. This justifies our assumption: taking into account $c\bar{c} - g$ absorption instead of charmonium disintegration in the nuclear matter would only strengthen J/Ψ suppression.

According to the above assumption, charmonium states can be absorbed first in the nuclear matter and soon later, when the matter appears in the CRR, in the hadron gas. Since these two processes are separate in time, J/Ψ survival factor for a heavy-ion collision with the initial energy density ϵ_0, may be written in the form

$$\mathcal{N}(\epsilon_0) = \mathcal{N}_{n.m.}(\epsilon_0) \cdot \mathcal{N}_{h.g.}(\epsilon_0) , \tag{6}$$

where $\mathcal{N}_{n.m.}(\epsilon_0)$ and $\mathcal{N}_{h.g.}(\epsilon_0)$ are J/Ψ survival factors in the nuclear matter and the hadron gas, respectively. For $\mathcal{N}_{n.m.}(\epsilon_0)$ we have the usual approximation [32–35]

$$\mathcal{N}_{n.m.}(\epsilon_0) \cong \exp\left\{ -\sigma_{\psi N} \rho_0 L \right\} , \tag{7}$$

where ρ_0 is the nuclear matter density and L the mean path length of the J/Ψ through the colliding nuclei. For the last quantity, we use the expression given in [35]:

$$\rho_0 L(b) = \frac{1}{2T_{AB}} \int d^2\vec{s}\, T_A(\vec{s}) T_B(\vec{s} - \vec{b}) \left[\frac{A-1}{A} T_A(\vec{s}) + \frac{B-1}{B} T_B(\vec{s} - \vec{b}) \right] , \tag{8}$$

where $T_{AB}(b) = \int d^2\vec{s}\; T_A(\vec{s})T_B(\vec{s}-\vec{b})$, $T_A(\vec{s}) = \int dz \rho_A(\vec{s},z)$ is the nuclear density profile function, $\rho_A(\vec{s},z)$ the nuclear matter density distribution (normalized to A) and b the impact parameter. How to obtain ϵ_0 as a function of b will be presented further.

To estimate $\mathcal{N}_{h.g.}(\epsilon_0)$ we follow the idea presented in [5], but now generalized to the case of the gas which consists of different species of particles. We shall focus on the plane $z = 0$ (z is a collision axis) and put J/Ψ longitudinal momentum equal to zero. Now the p_T-dependent J/Ψ survival factor $\mathcal{N}_{h.g.}(p_T)$ is given by (for details see [12])

$$\mathcal{N}_{h.g.}(p_T) = \int d^2\vec{s} f_0(s,p_T) \exp\left\{ - \int_{t_0}^{t_f} dt \sum_{i=1}^{l} \int \frac{d^3\vec{q}}{(2\pi)^3} f_i(\vec{q},t)\sigma_i v_{rel,i} \frac{p_\nu q_i^\nu}{E E_i'} \right\} , \tag{9}$$

where the sum in the power is over all taken species of scatters (hadrons), $p^\nu = (E, \vec{p}_T)$ and $q_i^\nu = (E_i', \vec{q})$ are four momenta of J/Ψ and hadron specie i respectively, $\vec{v} = \vec{p}_T/E$ is the velocity of the former, σ_i states for the absorption cross-section of $J/\Psi - h_i$ scattering and $v_{rel,i}$ is the relative velocity of h_i hadron with respect to J/Ψ. When M and m_i denote J/Ψ and h_i masses, respectively ($M = 3097$ MeV), $v_{rel,i}$ reads

$$v_{rel,i} = \left(1 - \frac{m_i^2 M^2}{(p_\nu q_i^\nu)^2} \right)^{\frac{1}{2}} . \tag{10}$$

The upper limit of the time integral in (9) , t_f, is equal to $t_{f.o.}$ or to t_{esc} – the moment of leaving by a given J/Ψ of the hadron medium, if the final-size effects are considered and $t_{esc} < t_{f.o.}$. For σ_i we have assumed that it equals zero for $(p^\nu + q_i^\nu)^2 < (2m_D + m_X)^2$ and is constant elsewhere (m_D is a charm meson mass, $m_D = 1867$ MeV). For hadron specie i we have usual Bose-Einstein or Fermi-Dirac distribution (we neglect any possible spatial dependence here)

$$f_i(\vec{q},t) = f_i(q,t) = \frac{2s_i + 1}{\exp\left\{ \frac{E_i' - \mu_i(t)}{T(t)} \right\} + g_i} . \tag{11}$$

In the following, we shall consider only J/Ψ initial distribution $f_0(s,p_T)$ that factorizes into $f_0(s)g(p_T)$ and the momentum distribution $g(p_T)$ will be given by (4) . We assume at the first step that the transverse size of the hadron medium is much greater than $t_{f.o.}$ and also much greater than the size of the area where $f_0(s)$ is non-zero. Additionally we assume that $f_0(s)$ is uniform and normalized to unity. Note that the first assumption overestimates the suppression but the second, in the presence of the first, has no any calculable effect here. As a result, $\mathcal{N}_{h.g.}(p_T)$ simplifies to

$$\mathcal{N}_{h.g.}(p_T) = g(p_T,\epsilon_0) \cdot \exp\left\{ - \int_{t_0}^{t_{f.o.}} dt \sum_{i=1}^{l} \int \frac{d^3\vec{q}}{(2\pi)^3} f_i(\vec{q},t)\sigma_i v_{rel,i} \frac{p_\nu q_i^\nu}{E E_i'} \right\} , \tag{12}$$

To obtain $\mathcal{N}_{h.g.}(\epsilon_0)$ one needs only to integrate (12) over p_T:

$$\mathcal{N}_{h.g.}(\epsilon_0) = \int dp_T\; g(p_T,\epsilon_0) \cdot \exp\left\{ - \int_{t_0}^{t_{f.o.}} dt \sum_{i=1}^{l} \int \frac{d^3\vec{q}}{(2\pi)^3} f_i(\vec{q},t)\sigma_i v_{rel,i} \frac{p_\nu q_i^\nu}{E E_i'} \right\} . \tag{13}$$

Now we would like to take the final-size effects and the transverse expansion into account in our model. To do this directly, we would have to come back to the formula given by (9) and integrate it, instead of (12) , over p_T. But this would involve a five-dimensional integral (the three-dimensional integral over $\vec{q}$ simplifies to the one-dimensional one, in fact) instead of the three-dimensional integral of (13). Therefore, we need to simplify in some way the direct method just mentioned above. We shall define an average time of leaving the hadron medium by J/Ψ's with the velocity v produced in an A-B collision at impact parameter b, $\langle t_{esc} \rangle (b,v)$. Then, if this quantity is less than $t_{f.o.}$, we will put it instead of $t_{f.o.}$ as the upper limit of the integral over t in (13).

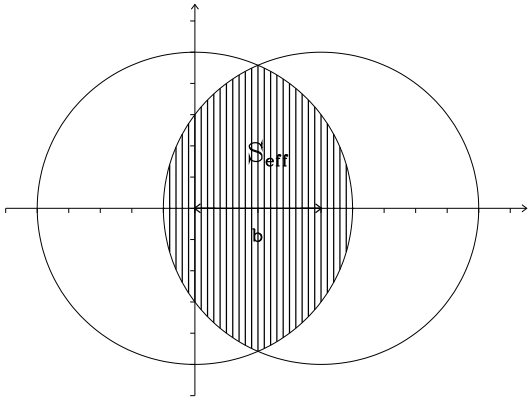

FIG. 2. View of a Pb-Pb collision at impact parameter b in the transverse plane ($z = 0$). The region where the nuclei overlap has been hatched and its area equals S_{eff}.

Let us consider an A-B collision at impact parameter b. Since we will compare final results with the latest data of NA50 which are for Pb-Pb collisions [14], we focus on the case of A=B here. So, for the collision at impact parameter b we have the situation in the plane $z = 0$ as presented in Fig. 2, where S_{eff} means the area of the overlap of the colliding nuclei. We shall assume here, that the hadron medium, which appears in the space between the nuclei after they crossed each other also has the shape of S_{eff} at t_0 in the plane $z = 0$. And additionally, the transverse expansion starts in the form of the rarefaction wave moving inward S_{eff} at t_0. Then, for a J/Ψ which is at $\vec{r} \in S_{eff}$ at the moment t_0 and has the velocity $\vec{v}$ we denote by t_{esc} the moment of crossing the border of the hadron gas. It means that t_{esc} is a solution of the equation $\mid \vec{d} + \vec{v}(t - t_0) \mid = R_A - c_s(t - t_0)$, where $R_A = r_0 \cdot A^{\frac{1}{3}}$ is the nucleus radius and $\vec{d} = \vec{r} - \vec{b}$ for the angel between $\vec{r}$ and $\vec{v}$ such that the J/Ψ will cross this part of the edge of the area of the hadron gas which was created by the projectile and $\vec{d} = \vec{r}$ in the opposite. Having obtained t_{esc}, we average it over the angel between $\vec{r}$ and $\vec{v}$, i.e. we integrate t_{esc} over this angel and divide by 2π. Then we average the result over S_{eff} with the weight given by

$$p_{J/\Psi}(\vec{r}) = \frac{T_A(\vec{r})T_B(\vec{r} - \vec{b})}{T_{AB}(b)} \tag{14}$$

and we obtain $\langle t_{esc} \rangle(b, v)$. So, the final expression for $\mathcal{N}_{h.g.}(\epsilon_0)$ when the transverse expansion is taken into account reads

$$\mathcal{N}_{h.g.}(\epsilon_0) = \int dp_T \; g(p_T, \epsilon_0) \cdot \exp\left\{ - \int_{t_0}^{t_{final}} dt \sum_{i=1}^{l} \int \frac{d^3\vec{q}}{(2\pi)^3} f_i(\vec{q}, t) \sigma_i v_{rel,i} \frac{p_\nu q_i^\nu}{E E_i'} \right\} \; , \tag{15}$$

where $t_{final} = min\{\langle t_{esc} \rangle, t_{f.o.}\}$.

IV. THE ENERGY DENSITY IN THE CRR

We compare our theoretical estimations for J/Ψ survival factor with the experimental data [14] presented as a function of ϵ_0. Usually, this quantity is estimated from the well-known Bjorken formula

$$\epsilon_0 = \frac{3 \cdot E_T}{\Delta\eta S_{eff} t_0} \; , \tag{16}$$

where $\Delta\eta$ is the pseudo-rapidity range and E_T is the neutral transverse energy.

In further considerations we will need the formula for the number of participating nucleons as a function of impact parameter b, which is given by the rough approximation (commonly used in the early nineties)

$$N_{part}(b) = \int_{S_{eff}} d^2\vec{s} \Big\{ T_A(\vec{s}) + T_B(\vec{s} - \vec{b}) \Big\} \; , \tag{17}$$

or in the term of the number of "wounded" nucleons [30,35]

$$N_{wound}(b) = \int d^2\vec{s}\, T_A(\vec{s}) \left\{ 1 - \left[1 - \frac{\sigma_N}{B} T_B(\vec{s} - \vec{b}) \right]^B \right\} + \int d^2\vec{s}\, T_B(\vec{s} - \vec{b}) \left\{ 1 - \left[1 - \frac{\sigma_N}{A} T_A(\vec{s}) \right]^A \right\} . \quad (18)$$

The both expressions are depicted in Fig. 3. Note that $N_{part}(b)$ is estimated for the uniform nuclear matter density with $r_0 = 1.2$ fm and $r_0 = 1.12$ fm, whereas $N_{wound}(b)$ is evaluated for the Woods-Saxon nuclear matter density distribution with parameters taken from [36]. With the use of $N_{wound}(b)$, the relation between E_T and b is established [30,35]

$$E_T = q \cdot N_{wound}(b) , \quad (19)$$

where $q = 0.4$ GeV. We could put (19) into (16) to obtain the dependence between ϵ_0 and b but the ratio $\frac{N_{wound}(b)}{S_{eff}(b)}$ is divergent when $b \to R_A + R_B$ (R_A and R_B are radii of a projectile and a target, respectively). From Fig. 3 we can see that in the case of Pb-Pb collisions, $N_{wound}(b)$ do not differ substantially from $N_{part}(b)$ with $r_0 = 1.2$ fm (besides the low b region). Therefore we can assume that for Pb-Pb collisions of NA50 the following approximation is valid:

$$E_T \cong q \cdot N_{part} . \quad (20)$$

Having put (20) into (16) we obtain ϵ_0 as a function of b

$$\epsilon_0(b) = \frac{N_{part}(b)}{S_{eff}(b)} , \quad (21)$$

where we have also used the value $\Delta\eta = 1.2$ of NA50 [14]. The above function is depicted in Fig. 4, together with $\epsilon_0(b)$ obtained from $\epsilon_0(E_T)$ with the use of (19). The dependence of ϵ_0 on E_T has been extracted directly from NA50 data [14].

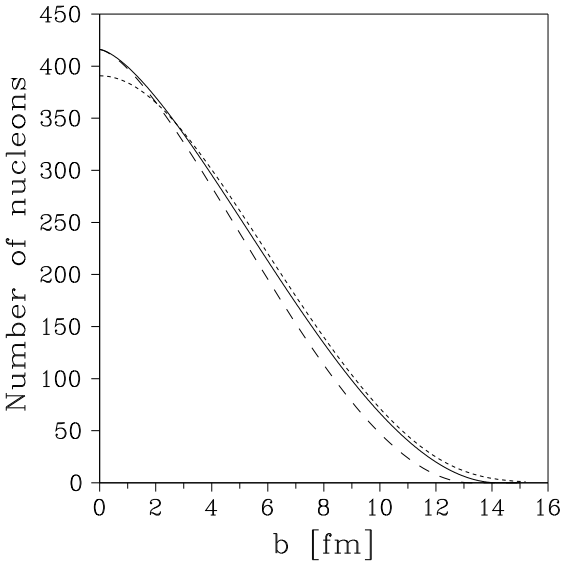

FIG. 3. Number of participating nucleons as a function of b for a Pb-Pb collision, estimated as: $N_{part}(b)$ for the uniform nuclear matter density and $r_0 = 1.2$ fm (solid), $r_0 = 1.12$ fm (dashed); $N_{wound}(b)$ for the Woods-Saxon distribution (short-dashed).

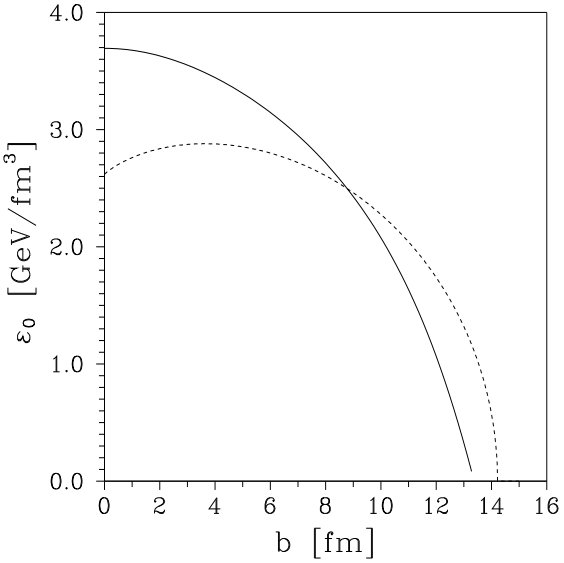

FIG. 4. The initial energy density ϵ_0 in the CRR for Pb-Pb collisions as the function of impact parameter b extracted from the NA50 data [14] (solid) and obtained from (21) (short-dashed).

We shall later see that the low b region (central collisions) is crucial for the understanding of experimental data. Also different plots in Fig. 4 will lead to different ranges of initial energy densities obtained from formula (21) or given by NA50 Collaboration [14].

V. RESULTS

To evaluate formulae (13) and (15) we have to know $T(t)$, $\mu_B(t)$ and $\mu_S(t)$ and how to obtain these functions was explained in Sect. II. But to follow all that procedure we need initial values s_0 and n_B^0. To estimate initial

baryon number density n_B^0 we can use experimental results for S-S [37] or Au-Au [10,38] collisions. In the first approximation we can assume that the baryon multiplicity per unit rapidity in the CRR is proportional to the number of participating nucleons. For a sulphur-sulphur collision we have $dN_B/dy \cong 6$ [37] and 64 participating nucleons. For the central collision of lead nuclei we can estimate the number of participating nucleons at $2A = 416$, so we have $dN_B/dy \cong 39$. Having taken the initial volume in the CRR equal to $\pi R_A^2 \cdot 1$ fm, we arrive at $n_B^0 \cong 0.25$ fm^{-3}. This is some underestimation because the S-S collisions were at a beam energy of 200 GeV/nucleon, but Pb-Pb at 158 GeV/nucleon. From the Au-Au data extrapolation one can estimate $n_B^0 \cong 0.65$ fm^{-3} [10]. These values are for central collisions, and for the higher impact parameter (a more peripheral collision) the initial baryon number density should be much lower. So, to simplify numerical calculations we will keep n_B^0 constant over the all range of b and additionally, to check the possible dependence on n_B^0, we will do our estimations for n_B^0 substantially lower, i.e. $n_B^0 = 0.05$ fm^{-3}.

Now, to find s_0, first we have to solve (2a - 2c) with respect to T, μ_S and μ_B, where we put $\epsilon = \epsilon_0$, $n_B = n_B^0$ and $n_S = 0$. Then, having put T, μ_S and μ_B into (2d) we obtain s_0. Finally, expressing left sides of (2b,2d) by (3) and after then solving (2b - 2d) numerically we can obtain T, μ_S and μ_B as functions of time. In fact, evaluating formulae (13) and (15) we do the following: first, we calculate $T = T(t)$ which turns out to be very well approximated by the expression

$$T(t) \cong T_0 \cdot t^{-a} \tag{22}$$

and then we put this approximation into (13) and (15) . And for $\mu_S(t)$ and $\mu_B(t)$ in $f_i(\vec{q}, t)$ we put solutions of (2b,2c) where n_B is given by (3), T by (22) and $n_S = 0$. But the exponent a in (22) has proven not to be unique for the whole range of T_0 considered here. One gets different values of the initial energy density ϵ_0 for different values of the impact parameter b and for different geometry of the collision process. So b dependent a gives also b dependent freeze-out time $t_{f.o}$. The density ϵ_0 is extracted from the dependence represented by the solid line in Fig. 4 for different values of b and Eqs. (2a - 2c) are solved. We have evaluated the suppression factor up to $\epsilon_0 = 3.7$ GeV/fm^3. This gives the maximal possible T_0, $T_{0,max}$, equal to 221.8 MeV (for $n_B^0 = 0.65$ fm^{-3}), 226 MeV (for $n_B^0 = 0.25$ fm^{-3}) or 226.7 MeV (for $n_B^0 = 0.05$ fm^{-3}).

This procedure allows to evaluate J/Ψ survival factor given by (13) . Because of the lack of data, we shall assume only two types of the cross-section, the first, σ_b, for J/Ψ-baryon scattering and the second, σ_m, for J/Ψ-meson scattering. For σ_b we put $\sigma_b = \sigma_{J/\psi N}$. As far as σ_m is concerned, we assume that this cross-section is 2/3 of the corresponding cross section for baryons, which is due to the quark counting. In the following, we will use values of $J/\Psi - Nucleon$ absorption cross-section $\sigma_{J/\psi N} \cong 3 - 5$ mb obtained from p-A data [15,27,32]. At the beginning, to illustrate how the value of power a influences J/Ψ suppression we present in Fig. 1 two results: the first for $a = \frac{1}{3}$ (what is the exact value for a free massless gas) and the second for $a = \frac{1}{5.6}$ (what is the approximate value for the hadron gas and $T_0 \cong 200$ MeV). We can see that the suppression improves more than twice for the highest ϵ_0 indeed.

To make our investigations more realistic we have to take into account that only about 60% of J/Ψ measured are directly produced during collision. The rest is the result of χ ($\sim 30\%$) and ψ' ($\sim 10\%$) decay [31]. Therefore the realistic J/Ψ survival factor should read

$$\mathcal{N}(\epsilon_0) = 0.6\mathcal{N}_{J/\psi}(\epsilon_0) + 0.3\mathcal{N}_{\chi}(\epsilon_0) + 0.1\mathcal{N}_{\psi'}(\epsilon_0) \ , \tag{23}$$

where $\mathcal{N}_{J/\psi}(\epsilon_0)$, $\mathcal{N}_{\chi}(\epsilon_0)$ and $\mathcal{N}_{\psi'}(\epsilon_0)$ are given also by formulae (4-15) but with $\langle p_T^2 \rangle_{J/\Psi}^{AB}(\epsilon) = \langle p_T^2 \rangle_{J/\Psi}^{AB}(\epsilon), \langle p_T^2 \rangle_{\chi}^{AB}(\epsilon), \langle p_T^2 \rangle_{\psi'}^{AB}(\epsilon)$, $K_{J/\psi} = K_{J/\psi}, K_{\chi}, K_{\psi'}$, $\sigma_{J/\psi N} = \sigma_{J/\psi N}, \sigma_{\chi N}, \sigma_{\psi' N}$ and $M = M_{J/\psi}, M_{\chi}, M_{\psi'}$ respectively. The remaining problem is whether formula (5) is valid for χ and ψ'. There are data for $\langle p_T^2 \rangle_{\psi'}^{PbPb}$ [39] and they shows that $\langle p_T^2 \rangle_{\psi'}^{PbPb} \approx 1.4 \langle p_T^2 \rangle_{J/\Psi}^{PbPb}$. So, we assume that the above is also true for $\langle p_T^2 \rangle_{\psi'}^{AB}(\epsilon)$, i.e.

$$\langle p_T^2 \rangle_{\psi'}^{AB}(\epsilon) = 1.4 \langle p_T^2 \rangle_{J/\Psi}^{AB}(\epsilon) \tag{24}$$

with $\langle p_T^2 \rangle_{J/\Psi}^{AB}(\epsilon)$ given by (5) . For χ we believe that the inequality

$$\langle p_T^2 \rangle_{J/\Psi}^{AB} \ \leq \ \langle p_T^2 \rangle_{\chi}^{AB} \ \leq \ \langle p_T^2 \rangle_{\psi'}^{AB} \tag{25}$$

should be valid and therefore assume that (24) is true also in this case. Anyway, the exact form of $\langle p_T^2 \rangle_{\chi}^{AB}(\epsilon)$ or $\langle p_T^2 \rangle_{\psi'}^{AB}(\epsilon)$ is not very important because we checked that the suppression depends on this form very weakly. First, we put $K_{J/\psi} = 0$ and the resulting J/Ψ survival factor (for direct J/Ψ's) differs only a few percent for the highest ϵ_0 from the one calculated with formula (5) unchanged. Second, when we use expression (5) also

for χ and ψ', the evaluated suppression factor is the same as that calculated with the use of (24), as far as plots are concerned.

To complete our estimations we need also values of cross-sections for $\chi - baryon$ and $\psi' - baryon$ scatterings (we will still hold that $\chi(\psi') - meson$ cross-section is $\frac{2}{3}$ of $\chi(\psi') - baryon$ cross-section). Since J/Ψ is smaller than χ or ψ', $\chi - baryon$ and $\psi' - baryon$ cross-sections should be greater than $J/\Psi - baryon$ one. For simplicity, we assume that all these cross-sections are equal. This means that we *underestimate* J/Ψ suppression, here. The final results of calculations of (13) are presented in Figs. 5-8 for various sets of parameters of our model (which are $T_{f.o.}, n_B^0, \sigma_b$). We performed these calculations for two values of $T_{f.o.} = 100, 140$ MeV which agree fairly well with values deduced from hadron yields [10]. For comparison, also the experimental data are shown in Figs. 5-8. The experimental survival factor is defined as

$$\mathcal{N}_{exp} = \frac{\frac{B_{\mu\mu}\sigma^{AB}_{J/\psi}}{\sigma^{AB}_{DY}}}{\frac{B_{\mu\mu}\sigma^{pp}_{J/\psi}}{\sigma^{pp}_{DY}}} \ , \tag{26}$$

where $\frac{B_{\mu\mu}\sigma^{AB(pp)}_{J/\psi}}{\sigma^{AB(pp)}_{DY}}$ is the ratio of the J/Ψ to the Drell-Yan production cross-section in A-B(p-p) interactions times the branching ratio of the J/Ψ into a muon pair. The values of the ratio for p-p, S-U and Pb-Pb are taken from [13,14]. Note that since the equality $\sigma^{AB}_{DY} = \sigma^{pp}_{DY} \cdot AB$ has been confirmed experimentally up to now [39], formula (26) reduces to

$$\mathcal{N}_{exp} = \frac{\sigma^{AB}_{J/\psi}}{AB\sigma^{pp}_{DY}} \ , \tag{27}$$

which is also given as the experimental survival factor, for instance, in [40].

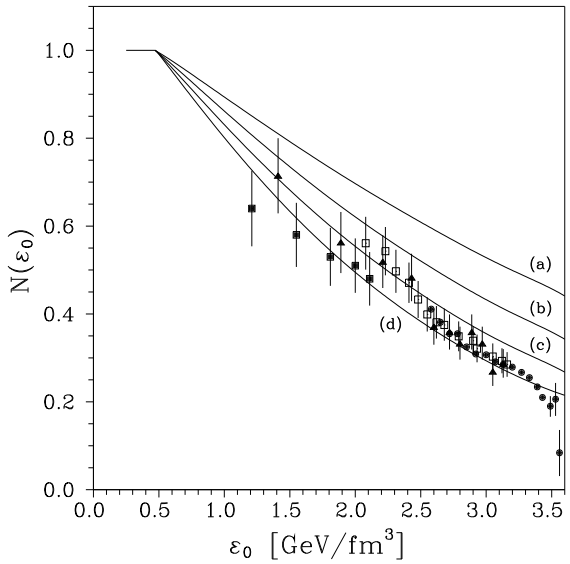

FIG. 5. J/Ψ suppression in the longitudinally expanding hadron gas with the "infinite" transverse size and for $n_B^0 = 0.25$ fm^{-3} and $T_{f.o.} = 140$ MeV: (a) $\sigma_b = 3$ mb, $\sigma_m = 2$ mb; (b) $\sigma_b = 4$ mb, $\sigma_m = 2.66$ mb; (c) $\sigma_b = 5$ mb, $\sigma_m = 3.33$ mb; (d) $\sigma_b = 6$ mb, $\sigma_m = 4$ mb . The black squares correspond to the NA38 S-U data [13], the black triangles correspond to the 1996 NA50 Pb-Pb data, the white squares to the 1996 analysis with minimum bias and the black points to the 1998 analysis with minimum bias [14].

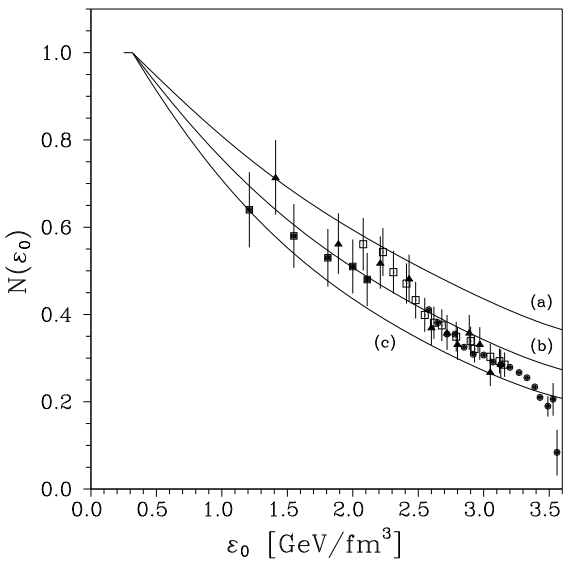

FIG. 6. Same as Fig. 5 (except case (d), which is not presented here) but for $T_{f.o.} = 100$ MeV.

Coming back to examination of our first results presented in Figs. 5-8, we can see that we have obtained patterns of suppression which agree with the experimental data fairly well for some values of parameters of our model. The data prefer $\sigma_b = 5 - 6$ mb and (or) $T_{f.o.}$ closer to 100 MeV. Note that the dependence on the

initial baryon number density is substantial but for higher values of n_B^0, rather. The lower the initial baryon number density, the deeper the suppression. There are two reasons for such a behaviour: the first, for the higher baryon number density, there are less non-strange heavier mesons ρ, ω in the hadron gas of the same ϵ_0, but these particles create the most weighty fraction of scatters, for which reaction (1) have no threshold at all; the second, the freeze-out time $t_{f.o.}$ decreases with increasing n_B^0 for a given ϵ_0 in our model. For instance, for $\epsilon_0 = 3.5$ GeV/fm^3 and $T_{f.o.} = 140$ MeV we have $a = 0.172,\ 0.175,\ 0.183$ and $t_{f.o.} = 15.7,\ 14.7,\ 11.6$ fm for $n_B^0 = 0.05,\ 0.25,\ 0.65$ fm^{-3}, respectively. We can see also that the value $\sigma_b = 3$ mb is too small to obtain results comparable with the data, so we will leave aside this value in further investigations.

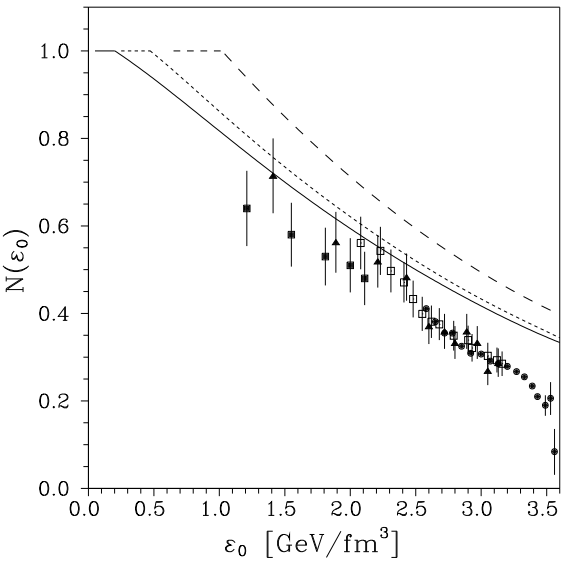

FIG. 7. J/Ψ suppression in the longitudinally expanding hadron gas with the "infinite" transverse size and for $\sigma_b = 4$ mb, $\sigma_m = 2.66$ mb and $T_{f.o.} = 140$ MeV. The curves correspond to $n_B^0 = 0.05$ fm^{-3} (solid), $n_B^0 = 0.25$ fm^{-3} (short-dashed) and $n_B^0 = 0.65$ fm^{-3} (dashed).The black squares represent the NA38 S-U data [13], the black triangles represent the 1996 NA50 Pb-Pb data, the white squares the 1996 analysis with minimum bias and the black points the 1998 analysis with minimum bias [14].

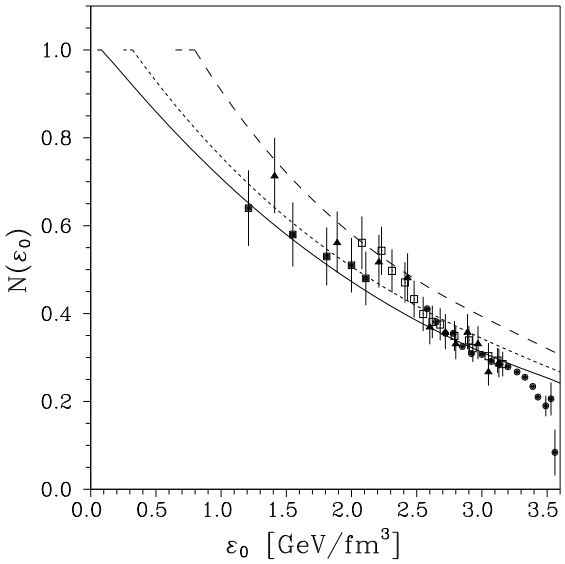

FIG. 8. Same as Fig. 7 but for $T_{f.o.} = 100$ MeV.

Now we will include the finite-size effects into our model, i.e. we will take into account that the realistic hadron gas has a finite transverse size. This will be done in form of the rarefaction wave moving inward S_{eff} with the sound velocity c_s. How to obtain this velocity has been mentioned in Sec.2 (see also [22]). With the finite-size effects included, the final expression for J/Ψ survival factor $\mathcal{N}_{h.g.}(\epsilon_0)$ will be given by (15) . To make our investigations much more realistic we will also include the possible J/Ψ disintegration in nuclear matter, which should increase J/Ψ suppression by about 10% [15]. But to draw also S-U data in figures, instead of multiplying $\mathcal{N}_{h.g.}$ by $\mathcal{N}_{n.m.}$ given by (7), we divide $\mathcal{N}_{exp}$ by appropriate $\mathcal{N}_{n.m.}$, i.e. we define "the experimental J/Ψ hadron gas survival factor" as

$$\tilde{\mathcal{N}}_{exp} = \exp\left\{\sigma_{J/\psi N}\rho_0 L\right\} \cdot \mathcal{N}_{exp} \ . \tag{28}$$

and values of this factor are drawn in Figs. 9-10 and Figs. 12-13 as the experimental data.

We shall consider the Woods-Saxon nuclear matter density distribution [36], here. The results of numerical estimations of (15) and (28) are depicted in Figs. 9-10 for two values of the charmonium-baryon cross-section $\sigma_b = 4,\ 5$ mb and the initial baryon number density $n_B^0 = 0.25,\ 0.65$ fm^{-3}. The curves for $n_B^0 = 0.05$ fm^{-3} almost cover the curves for $n_B^0 = 0.25$ fm^{-3}, so for clearness of the figure we do not draw them. The two values of the speed of sound are the maximal values of this quantity possible in the range $[T_{f.o.} = 140$ MeV, $T_{0,max}]$ for the above-mentioned two cases of n_B^0. In fact, we have checked that the results almost do not depend on c_s allowed in the range.

It has turned out also that in the case of the transverse expansion, the results almost do not depend on the $T_{f.o.}$ (for $T_{f.o.} \in [100, 140]$ MeV). This is because the freeze-out time resulting from the transverse expansion,

$t_{f.o.,trans} = R_A/c_s$ (if we assume a central collision and c_s constant), is of the order of the freeze-out time resulting from the longitudinal expansion for $T_{f.o.} = 140$ MeV. Namely, for Pb and $c_s = 0.45$ we have $t_{f.o.,trans} \cong 15.8$ fm, which is very similar to values of $t_{f.o.}$ for $T_{f.o.} = 140$ MeV given earlier. For $T_{f.o.} = 100$ MeV, $t_{f.o.} = 111.0,\ 101.0,\ 72.5$ fm for $n_B^0 = 0.05,\ 0.25,\ 0.65$ fm^{-3} respectively, so the hadron gas ceases because of the transverse expansion much earlier.

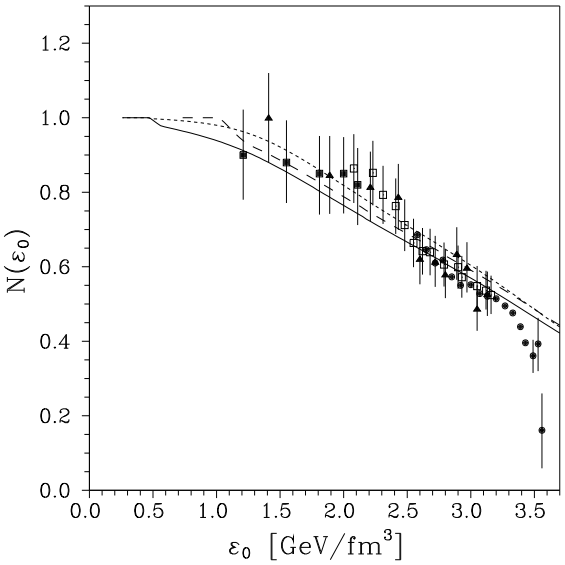

FIG. 9. J/Ψ suppression in the longitudinally and transversely expanding hadron gas for the Woods-Saxon nuclear matter density distribution and $\sigma_b = 4$ mb, $\sigma_m = 2.66$ mb and $T_{f.o.} = 140$ MeV. The curves correspond to $n_B^0 = 0.25$ fm^{-3}, $c_s = 0.45$, $r_0 = 1.2$ fm (solid), $n_B^0 = 0.65$ fm^{-3}, $c_s = 0.46$, $r_0 = 1.2$ fm (dashed) and $n_B^0 = 0.25$ fm^{-3}, $c_s = 0.45$, $r_0 = 1.12$ fm (short-dashed). The black squares represent the NA38 S-U data [13], the black triangles represent the 1996 NA50 Pb-Pb data, the white squares the 1996 analysis with minimum bias and the black points the 1998 analysis with minimum bias [14], but the data are "cleaned out" from the contribution of J/Ψ scattering in the nuclear matter in accordance with (28).

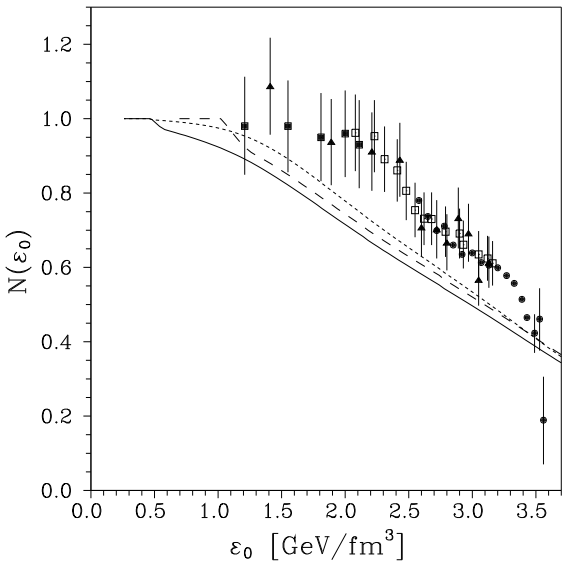

FIG. 10. Same as Fig. 9 but for $\sigma_b = 5$ mb and $\sigma_m = 3.33$ mb.

Generally, taking into account also the transverse expansion changes the final (theoretical) pattern of J/Ψ suppression qualitatively. First of all, the curves for the case including the transverse expansion are not convex, in opposite to the case with the longitudinal expansion only, where the curves are. But still, theoretical curves do not fall steep enough at high ϵ_0 to cover the data area completely. Nevertheless, from Figs. 9-10 we can see that for some choice of parameters, namely for σ_b somewhere between 4 and 5 mb and for $r_0 = 1.12$ fm, we would obtain a quite satisfactory curve. And we should remember that since we have one overall charmonium-baryon cross-section σ_b, our final results underestimate the suppression (for $\chi-,\ \psi' - baryon$ scattering the cross-section should be greater than for J/Ψ). To support our conclusion in more visible way we present main results from Figs. 9-10 in Fig. 11, where original data [14] for $\frac{B_{\mu\mu}\sigma^{PbPb}_{J/\psi}}{\sigma^{PbPb}_{DY}}$ and J/Ψ survival factors given by (6) multiplied by $\frac{B_{\mu\mu}\sigma^{pp}_{J/\psi}}{\sigma^{pp}_{DY}}$ and now as functions of E_T are presented. The change of the variable from ϵ_0 to E_T has been done with the use of (19) and $\epsilon_0 = \epsilon_0(b)$ expressed by the solid line in Fig. 4.

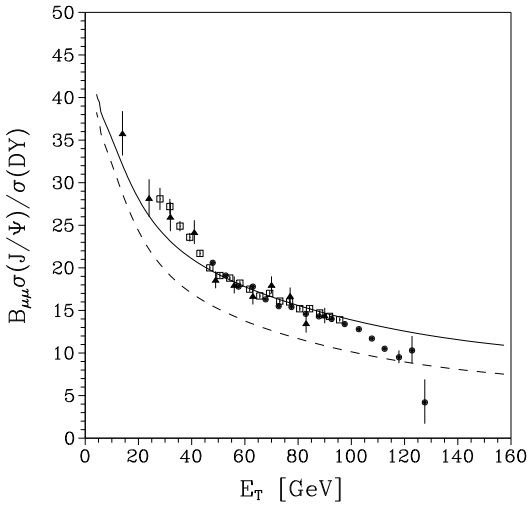

FIG. 11. J/Ψ survival factor times $\frac{B_{\mu\mu}\sigma^{pp}_{J/\psi}}{\sigma^{pp}_{DY}}$ in the longitudinally and transversely expanding hadron gas for the Woods-Saxon nuclear matter density distribution and $n_B^0 = 0.25$ fm^{-3}, $T_{f.o.} = 140$ MeV, $c_s = 0.45$ and $r_0 = 1.2$ fm. The curves correspond to $\sigma_b = 4$ mb (solid) and $\sigma_b = 5$ mb (dashed). The black triangles represent the 1996 NA50 Pb-Pb data, the white squares the 1996 analysis with minimum bias and the black points the 1998 analysis with minimum bias [14].

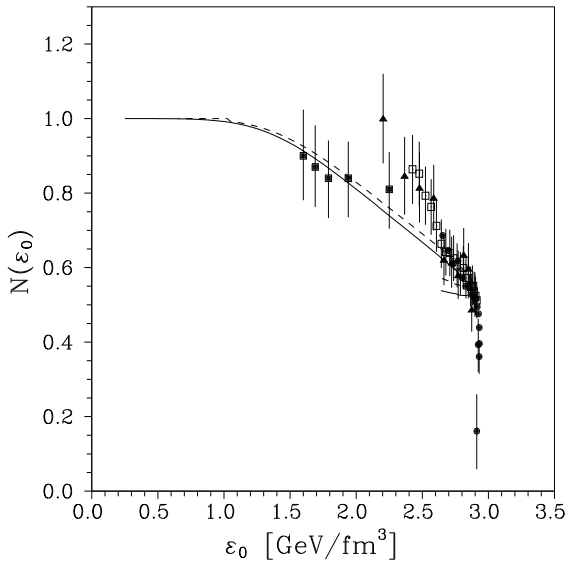

FIG. 12. J/Ψ suppression in the longitudinally and transversely expanding hadron gas for the Woods-Saxon nuclear matter density distribution and $\sigma_b = 4$mb, $\sigma_m = 2.66$ mb, $T_{f.o.} = 140$ MeV and $r_0 = 1.2$ fm but for $\epsilon_0(b)$ given by (21). The curves correspond to $n_B^0 = 0.25$ fm^{-3}, $c_s = 0.45$ (solid) and $n_B^0 = 0.65$ fm^{-3}, $c_s = 0.46$ (dashed). The black squares represent the NA38 S-U data [13], the black triangles represent the 1996 NA50 Pb-Pb data, the white squares the 1996 analysis with minimum bias and the black points the 1998 analysis with minimum bias [14], but the data are "cleaned out" from the contribution of J/Ψ scattering in the nuclear matter in accordance with (28).

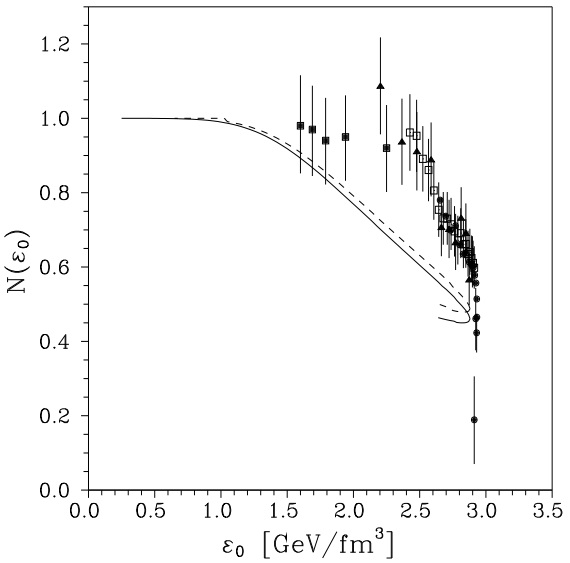

FIG. 13. Same as Fig. 12 but for $\sigma_b = 5$ mb and $\sigma_m = 3.33$ mb.

Note that the main disagreement with the data reveals in the last experimental point of the 1998 analysis

[14] (see Figs. 5-11). But the error bar of this point is very wide. Additionally, there is some contradiction in positions of the last three points of the 1998 data. In fact, the middle point goes up above the left one and the last falls far below the two earlier. This suggests that more experimental data is needed in the region of high ϵ_0 to state definitely whether the abrupt fall of the experimental suppression factor takes place or not there.

Now we repeat again the numerical estimations of (15) for the case with the finite-size effects and the Woods-Saxon nuclear matter density distribution included, but for the dependence of ϵ_0 on b given by (21). The results are presented in Figs. 12-13. Note that the theoretical curves are two-valued around $\epsilon_0 = 2.8$ GeV/fm^3. This is the result of our approximation of $\epsilon_0(b)$ by (21). This expression allows for two different values of b, which give the same ϵ_0 in some range of the impact parameter b. This is shown in Fig. 4 (short-dashed line). We can see that for $b \leq 7.9$ fm there are two different values b_1 and b_2 such that $\epsilon_0(b_1) = \epsilon_0(b_2)$. This causes that results plotted in Figs. 12-13 are qualitatively different from those presented in Figs. 9-10 in the region close to the maximal ϵ_0 reached at the collision. Comparing Figs. 9-10 with Figs. 12-13, we can see also that the pattern of J/Ψ suppression depends on the shape of ϵ_0 as a function of b. Clarification of this dependence would be very helpful to obtain more realistic picture of the J/Ψ dissociation in hadron medium during the heavy-ion collisions.

As a final remark, we think that it is difficult to exclude J/Ψ scattering in the hot hadron gas entirely, as the reason for the observed J/Ψ suppression at this point (see also [41]). In our model the most crucial parameter is the *charmonium−baryon* inelastic cross-section and the final results depend on its value substantially. Therefore it is of the greatest importance to establish how this cross-section behaves in the hot hadron environment. Some work has been done into this direction [42–44], but results presented there differ from each other and are based on different models. However, the newest estimations of $\pi + J/\Psi$, $\rho + J/\Psi$ and $J/\Psi + N$ cross-sections at high invariant collision energies [45,46] agree with the values of σ_b and σ_m assumed in our model. We would like to add also at this point that the $charmonium - hadron$ inelastic cross-sections have been considered as constant quantities here. For sure, they should not be constant and the results of just mentioned papers [45,46] suggests that they are not, indeed. They are growing functions of the invariant collision energy $\sqrt{s}$. So, the naive reasoning should direct us to the conclusion that the increase of ϵ_0 (or in other words E_T) causes the increase of the invariant collision energy $\sqrt{s}$ on the average and further the increase of the $charmonium - hadron$ inelastic cross-sections. This could influence the final patterns of J/Ψ suppression in such a way that J/Ψ survival factor would behave according to the solid curve of Fig. 11 for low ϵ_0 (E_T) but then, as the $charmonium - hadron$ inelastic cross-sections would increase with ϵ_0 (E_T), the factor would go closer to the dashed curve of Fig. 11 for high ϵ_0 (E_T). So, the experimental pattern of J/Ψ suppression could be recovered in this way. Therefore, as a final conclusion we can say that it is difficult to ruled out the conventional explanations of J/Ψ suppression completely, at present.

We would like to stress again that the behaviour of the experimental J/Ψ suppression factor at high E_T (or otherwise at high ϵ_0) has not been clear yet. In fact, the abrupt fall of this factor (what could suggest the appearance of the quark-gluon plasma) is indicated only by the one point (the last) of the 1998 NA50 analysis [14]. So, to draw a definite conclusion more experimental data far above $E_T = 120$ GeV are needed. This region will be reached in upcoming RHIC runs and their results should answer the question: is the J/Ψ suppression a signature of the existence of the quark-gluon plasma, or not?.

Note added. When our paper was completed we became aware of [47] where the twin figure (denoted as Fig.5 there) to our Fig. 11 was presented. But the appearance of the quark-gluon plasma is the main reason for J/Ψ suppression there. It is also claimed that results shown in that figure "provide evidence for the production of the quark-gluon plasma in central high-energy Pb-Pb collisions". This entirely confirms our conclusion that the status of J/Ψ suppression as a signal for the quark-gluon plasma appearance is far from being clear at present.

ACKNOWLEDGMENTS

We would like to thank Dr K. Redlich for very helpful discussions.
Work supported in part by the Polish Committee for Scientific Research under contract KBN-2 P03B 030 18 .

[1] T. Matsui and H. Satz, Phys. Lett. **B178**, 416 (1986).
[2] J.Ftáčnik, P.Lichard and J.Pišút, Phys. Lett. **B207**, 194 (1988).

[3] R. Vogt, M. Prakash, P. Koch and T. H. Hansson, Phys. Lett. **B207**, 263 (1988).
[4] S. Gavin, M. Gyulassy and A. Jackson, Phys. Lett. **B207**, 257 (1988).
[5] J. P. Blaizot and J. Y. Ollitrault, Phys. Rev. D **39**, 232 (1989).
[6] R. Vogt, Phys. Rept. **310**, 197 (1999).
[7] F. Karsch, hep-ph/0103314; Nucl. Phys. Proc. Suppl. **83**, 14 (2000) [hep-lat/9909006].
[8] E. L. Bratkovskaya, W. Cassing, C. Greiner, M. Effenberger, U. Mosel and A. Sibirtsev, Nucl. Phys. **A675**, 661 (2000) [nucl-th/0001008].
[9] R. Hagedorn, Nuovo Cim. Suppl. **3**, 147 (1965); R. Hagedorn, *In *Erice 1972, Proceedings, Study Institute On High Energy Astrophysics*, Cambridge 1974, 255-296.*
[10] J. Stachel, Nucl. Phys. **A654**, 119C (1999) [nucl-ex/9903007].
[11] L. V. Bravina *et al.*, Phys. Rev. **C 60**, 024904 (1999) [hep-ph/9906548].
[12] D. Prorok and L. Turko, Z. Phys. **C61**, 109 (1994).
[13] M.C. M. C. Abreu *et al.* [NA38 Collaboration], Phys. Lett. **B449**, 128 (1999); M. C. Abreu *et al.*, Phys. Lett. **B466**, 408 (1999).
[14] M. C. Abreu *et al.* [NA50 Collaboration], Phys. Lett. **B450**, 456 (1999); M. C. Abreu *et al.* [NA50 Collaboration], Phys. Lett. **B477**, 28 (2000).
[15] C. Gerschel, J. Hüfner, Phys. Lett. **B207**, 253 (1988).
[16] S. Gavin and R. Vogt, Nucl. Phys. **B345**, 104 (1990).
[17] S. J. Brodsky and A. H. Mueller, Phys. Lett. **B206**, 685 (1988).
[18] J. D. Bjorken, Phys. Rev. D **27**, 140 (1983).
[19] R. Bellwied, H. Caines and T. J. Humanic, Phys. Rev. **C62** (2000) 054906 [hep-ph/0003264].
[20] G. Baym, B. L. Friman, J. P. Blaizot, M. Soyeur and W. Czyż, Nucl. Phys. **A407**, 541 (1983).
[21] D. Prorok and L. Turko, Z. Phys. **C68**, 315 (1995) [hep-ph/9411250].
[22] D. Prorok and L. Turko, hep-ph/0101220.
[23] J. Cleymans, R. V. Gavai and E. Suhonen, Phys. Rept. **130**, 217 (1986).
[24] J. Hufner, Y. Kurihara and H. J. Pirner, Phys. Lett. **B215**, 218 (1988).
[25] S. Gavin and M. Gyulassy, Phys. Lett. **B214**, 241 (1988).
[26] J. P. Blaizot and J. Y. Ollitrault, Phys. Lett. **B217**, 392 (1989).
[27] J. Badier *et al.* [NA3 Collaboration], Z. Phys. **C20**, 101 (1983).
[28] S. Gupta and H. Satz, Phys. Lett. **B283**, 439 (1992).
[29] C. Baglin *et al.* [NA38 Collaboration], Phys. Lett. **B268**, 453 (1991).
[30] D. Kharzeev, C. Lourenço, M. Nardi and H. Satz, Z. Phys. **C74**, 307 (1997) [hep-ph/9612217].
[31] H. Satz, hep-ph/9711289.
[32] S. Gavin and R. Vogt, Phys. Rev. Lett. **78**, 1006 (1997) [hep-ph/9606460].
[33] C. Gerschel and J. Hüfner, Z. Phys. **C56**, 171 (1992).
[34] S. Gavin, hep-ph/9609470.
[35] F.Bellaiche, PhD Thesis, Université Claude Bernard Lyon-I, Lyon, 1997; F.Fleuret, PhD Thesis, Ecole Polytechnique, Palaiseau, 1997
[36] C. W. de Jager, H. de Vries, C. de Vries, Atomic Data and Nuclear Data Tables **14**, 479 (1974)
[37] J. Baechler *et al.* [NA35 Collaboration], Nucl. Phys. **A525**, 59C (1991).
[38] L. Ahle *et al.* [E802 Collaboration], Phys. Rev. C **57**, R466 (1998).
[39] M. C. Abreu *et al.* [NA50 Collaboration], Nucl. Phys. **A638**, 261C (1998).
[40] C. Lourenço, Nucl. Phys. **A610**, 552C (1996) [hep-ph/9612222].
[41] A. Capella, E. G. Ferreiro and A. B. Kaidalov, Phys. Rev. Lett. **85**, 2080 (2000) [hep-ph/0002300].
[42] D. Kharzeev and H. Satz, Phys. Lett. **B334**, 155 (1994) [hep-ph/9405414].
[43] K. Martins, D. Blaschke and E. Quack, Phys. Rev. C **51**, 2723 (1995) [hep-ph/9411302].
[44] S. G. Matinian and B. Müller, Phys. Rev. C **58**, 2994 (1998) [nucl-th/9806027].
[45] K. Tsushima, A. Sibirtsev, K. Saito, A. W. Thomas and D. H. Lu, Nucl. Phys. **A680**, 279 (2000) [nucl-th/0005065].
[46] A. Sibirtsev, K. Tsushima and A. W. Thomas, nucl-th/0005041.
[47] C. Wong, Nucl. Phys. A **681**, 22 (2001) [nucl-th/0007046].